Detection of Shot Noise in Solar Cells and LEDs Using Cross-Correlation Current Noise Spectroscopy

Kevin Davenport
Department of Physics and Astronomy
Univeristy of Utah Salt Lake City, UT, USA
kevin.davenport@utah.edu

Mark Hayward
Department of Physics and Astronomy
Univeristy of Utah Salt Lake City, UT, USA

Andrey Rogachev
Department of Physics and Astronomy
University of Utah
Salt Lake City, UT, USA

***Abstract*—Using cross-correlation techniques, we are able to extend the bandwidth of typical noise measurements and go beyond the standard 1/f characterization of heterostructured silicon and perovskite solar cells, as well as organic light-emitting diodes. With this method, we are able to resolve the frequency-independent contribution to the noise spectra. In all studied systems, we find this term to be roughly proportional to current and, therefore, attributed to shot noise. The extracted Fano factor, F, from the equation *S = 2eIF*, was found to be in the range 0.2-1. We argue that in the solar cells, this shot noise originates from discreteness of electron-hole pair generation by photons and from discreteness of tunneling of charge carriers across internal interfacial barriers. In organic LEDs, the shot noise is likely due to bottleneck effects related to bulk percolative transport.**

Keywords—noise, cross-correlation, solar cell, organic LED, shot noise, Fano factor

I. Introduction

Noise spectroscopy has proven an effective tool over the last several decades for studying transport dynamics and defect states [1,2] in both organic and inorganic materials and devices [3,4]. However, much of this literature focuses on low-frequency flicker noise below 10kHz [5]. The primary limitation is twofold: (i) the background noise of the front amplifiers in single-channel spectrum analyzers set the noise floor, limiting viewable signal, and (ii) in devices with planar geometry, their capacitance leads to a high-frequency roll-off in voltage noise measurements, which is often indistinguishable from 1/*f* noise.

We have designed and constructed a two-channel spectrum analyzer based on the current cross-correlation technique [6,7]. This allows us to resolve details in noise spectra well below the noise floor. The transimpedance stage has been built in close proximity (>1cm) to the device under test, greatly reducing parasitic input capacitance, thus increasing bandwidth. In an improvement over our apparatus used in earlier noise [8,9] and impedance [10,11] studies of organic LEDs, the first amplification stage has been built inside a liquid nitrogen flow cryostat with optical access. This allows noise spectra to be collected under different light intensities, device currents, and temperatures.

II. Experimental

Here we report the study of three different types of devices: a series of high-efficiency silicon solar cells, the structure of which is shown in Fig. 3; methylammonium lead triiodide perovskite solar cells, shown in Fig. 5; and a series of super yellow PPV co-polymer organic light emitting diodes, shown in Fig. 7. All devices were studied under vacuum, using current noise measurements as detailed in [7] under zero bias conditions. Illumination was provided by a high-power, broad spectrum light-emitting diode powered using batteries. For the solar cells, a yellow LED ($\lambda = 585-595nm$) was used. For the super yellow samples, a blue LED ($\lambda = 450-465nm$) was used to excite above the bandgap. The output of the transimpedance stage was first sent through a custom-built two-stage, low-noise amplifier and then into a National Instruments 6366 USB DAQ card. The cross-correlation was performed in a computer with a purpose-built LabVIEW procedure.

III. Results and Discussion

A. Detection of Shot Noise

We found that in the three studied series of devices, all contributions to noise spectra can be accounted for by some (or all) of the terms in the following equation:

$$S = S_1 + \frac{S_2}{f^a} + S_3 \times \mathrm{Re}\left[\frac{1}{1+(i\omega\tau)^{1-b}}\right] + S_4 f^c. \qquad (1)$$

Here, the first term represents a frequency-independent noise contribution made up of shot noise, thermal noise, and residual background noise. The second term represents the contribution of 1/*f*-like flicker noise. The third term is a generic generation-recombination noise which allows for a distribution of recombination times, τ; note that if $b = 0$, this term takes on the familiar Lorentzian form for a single recombination time. Finally, the fourth term represents an upturn due to sample capacitance which cannot be removed by the cross-correlation method. Ideally, $c = 2$ [7], though we often find a value that is between 1.5 and 2 due to noise gain peaking [14].

An important technical achievement of our work is the ability to resolve shot noise (S_1 term) in planar devices with large capacitances. The total shot noise in these devices can be thought of as generated by a series of noise sources, each self-shorted by its resistance, R_n (Fig. 1) [12]. These resistances model the energy barriers encountered by charge carriers at the interfaces between materials, or between hopping sites along a percolative transport path.

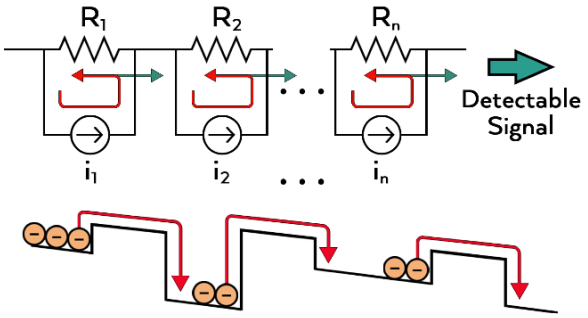

Fig. 1. Shot noise sources envisioned as a collection resistive Kirchhoff loops, each corresponding to an internal energy barrier. These could be seen as tunneling barriers, such as at the interfaces between materials, or as percolation hopping sites.

From Kirchhoff's law, the total noise current is given as

$$I_T = \sum_n \frac{i_n R_n}{R_T}, \qquad (2)$$

where R_T is the total resistance of a given device. As a first approximation, the current noise sources are uncorrelated and each of them generates full scale shot noise power with the Schottky value $S_n = 2eI$. The total shot noise seen by the electrodes then is

$$S_T = \left\langle I_T^2 \right\rangle = \sum_n \left\langle i_n^2 \right\rangle \left(\frac{R_n}{R_T} \right)^2 = 2eI \sum_n \left(\frac{R_n}{R_T} \right)^2 = 2eIF, \qquad (3)$$

where the Fano factor, F, characterizes the reduction of the noise. Thus, the addition of sources to the network actually suppresses the overall shot noise signal. For example, for N identical noise sources in series, $F = 1/N$.

B. Shot noise in silicon solar cells

Fig. 2a below shows the current noise spectra of a high-efficiency silicon solar cell. At the bottom of the Fig.3 the structure of the device is shown. The bulk of this device is a 145 μm-thick layer of n-type crystalline silicon (Cz-Si) grown via the Czochralski process. Very narrow layers of p-doped amorphous Si and n-doped nanocrystalline Si (energy gap 1.6 eV) allow efficient light propagation into the Cz-Si where the generation of electron-hole pairs takes place. These layers have a high concentration of defects; to separate them from the Cz-Si, two passivating layers of hydrogenated intrinsic amorphous Si (i-α-Si:H) have been deposited on both sides. The p-n junction of the device extends over three layers: the n-Cz-Si, i-α-Si:H, and p-α-Si:H. Finally, a thin layer of ITO and gold contacts have been deposited on either side. The total area of the device is 1 cm^2. In our experiment, the sample was illuminated from the side of the p-type material, however illumination from the either side yields similar efficiency.

The noise spectra shown in Fig.1 were taken in the short circuit configuration; the legend indicates light-induced DC current in the device. The solid lines show Eq.1 fit to the data.

The mid-frequency feature, seen from approximately 1kHz to 100kHz, is the result of the combination of the frequency-independent and generation-recombination noise contributions; this feature is completely hidden in the single channel data. Similar to [8], all of the terms in Eq. 1 are necessary to acquire a good fit to the data.

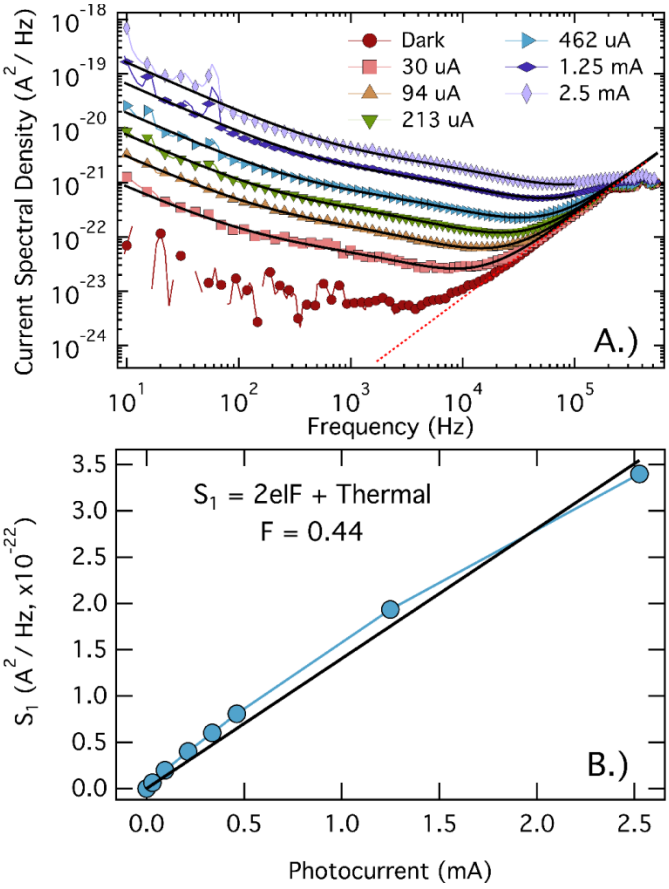

Fig. 2. A.) Cross-correlated current noise spectral density curves for an amorphous silicon photovoltaic cell at 0V bias under different illuminations at 300K. Black curves represent a fit to Eq. 1. The red dashed line represents the residual capacitive upturn. B.) The frequency-independent term extracted from the fit, showing a Fano Factor of $F = 0.44$

Fig. 2b shows the magnitude of the frequency-independent term plotted as a function of photocurrent, the linear dependence of which indicates that this term is due to shot noise. From the fit, shown in black, we find a Fano factor of $F = 0.44$

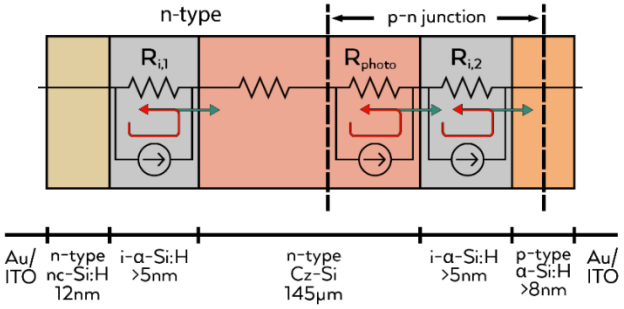

Fig. 3. Equivalent circuit and device structure (not to scale) of the silicon solar cells studied. The main generators of shot noise are likely the highly-resistive intrinsic amorphous silicon layers surrounding the bulk, one of which is additionally modified by the presence of a p-n junction.

Based on the model presented in section A, we can identify three main sources of shot noise (Fig. 3). Out of these, the likely dominant sources are the thin, intrinsic silicon layers which serve to passivate surface defect states on the bulk Cz-Si layer; these intrinsic layers are much more resistive than the doped layers, 10^{-9} S/cm compared to 10^{-3} S/cm. If the two layers were identical, a Fano factor of $F = 0.5$ would be expected. Deviation from this value can occur for two reasons. First, one of the intrinsic layers lies inside the device p-n junction, modifying the layer's net resistance and thus contributing asymmetrically to the Fano factor. Second, the internal resistance of the bulk layer increases the value of the total device resistance, R_T, which pushes the Fano factor below 0.5.

C. Shot noise in perovskite solar cells

Fig. 4a shows current noise spectra, along with their fits to Eq. 1, for a perovskite solar cell. The structure of the device is show in Fig.5. A TiO_2 matrix was deposited on top of an FTO-templated glass substrate, upon which approximately 100 µm of the organic-inorganic hybrid perovskite methylammonium lead triiodide was added via spin coating. The hole transport material spiro-OMeTAD was then deposited, also using spin coating, followed by the thermal evaporation deposition of the gold contact. Each glass substrate contained four separate devices, each ~25mm^2.

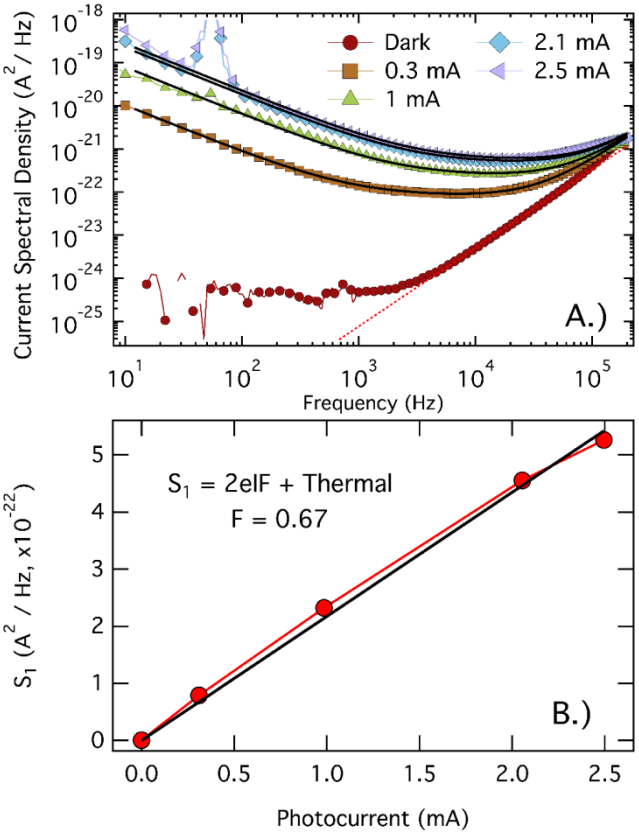

Fig. 4. A.) Cross-correlated current noise spectral density curves for a perovskite photovoltaic cell at 0V bias under different illuminations at 300K. Black curves represent a fit to Eq. 1. The red dashed line represents the residual capacitive upturn. B.) The frequency-independent term extracted from the fit, showing a Fano Factor of $F = 0.67$

Comparing these data to those in Fig. 2a, we see the absence of the generation-recombination term seen in the silicon samples.

The magnitude of the S_1 term extracted from the fits here is roughly the same order of magnitude (~10^{-22}) as that seen in the silicon samples, however the extracted Fano Factor is $F = 0.67$. The equivalent circuit for the perovskites (Fig. 5) is simpler than that of silicon due to a less complex internal structure.

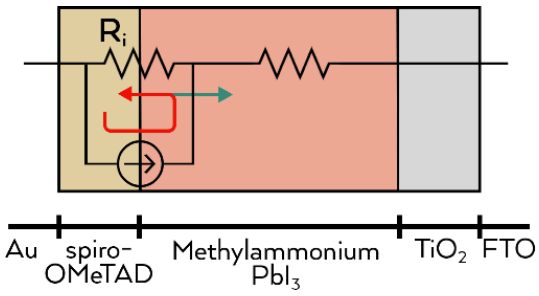

Fig. 5. Equivalent circuit and device structure of the perovskite solar cells studied. The main shot noise generator is likely the modified interface between the spiro-OMeTAD hole transport layer and the methylammonium PbI_3 interface.

It has been observed that performance degradation can occur in these devices due to the modification of the spiro-OMeTAD transport layer [13], either through direct modification such as photo-oxidization, or by diffusion of Au from the anode contact. Therefore, it seems likely that this layer is responsible for the generation of shot noise in these devices. The fact that F>0.5 supports this claim as a greater number of barriers would drop this below 0.5, as seen in the silicon devices.

D. Shot noise in super yellow PPV co-polymer LEDs

Fig. 6a shows current noise spectra collected from a super yellow LED operated as a photovoltaic cell. The structure of the device is indicated in Fig. 7. Approximately 100 nm of PEDOT:PSS was spin coated onto an ITO-patterned glass substrate, followed by 50 nm of super yellow PPV co-polymer. An anode of calcium and aluminum was then deposited via thermal evaporation. The device active area is ~1mm^2.

The properties which make for a good LED tend to be at odds with the desired properties of a good photovoltaic. LEDs are designed to promote exciton formation and recombination, whereas the desirable trait in a photovoltaic is rapid and efficient exciton dissociation. This is reflected in the data by the fact that the observed short circuit current seen in the super yellow devices was many orders of magnitude lower than either of the solar cell samples, even at much higher illumination intensities.

The small currents led to a lower signal-to-noise ratio, making curve fitting more difficult. The dashed lines in Fig. 6a represent a fit to the mid-frequency plateau region which corresponds to the upper bound of the frequency-independent term. The qualitative shape of the curves suggests that the generation-recombination term is not present, similar to the perovskites.

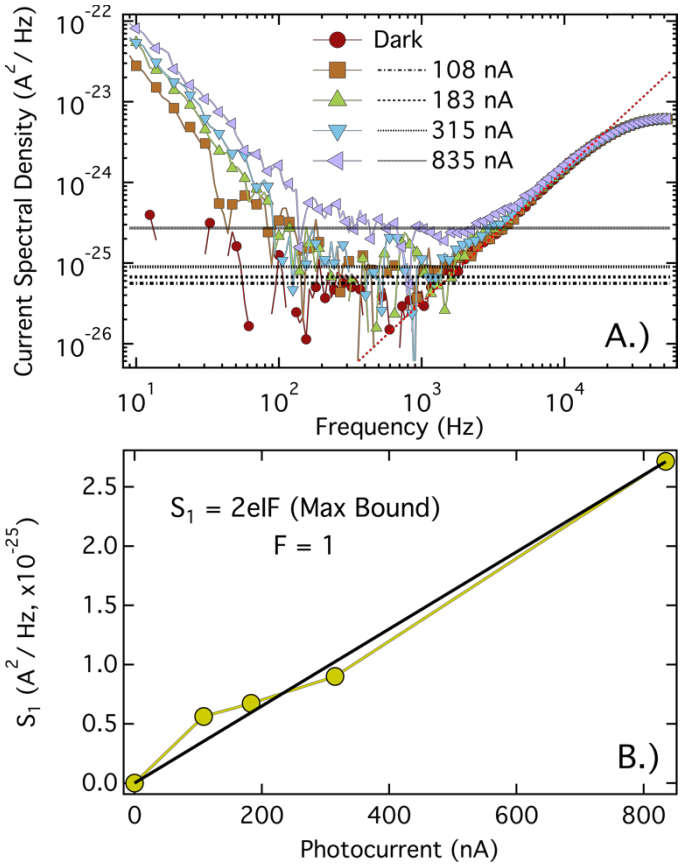

Fig. 6. Cross-correlated current noise spectral density curves for a super yellow PPV co-polymer LED, operated as a photovoltaic, at 0V bias under different illuminations at 300K. The dashed lines represent a fit to the noise plateau corresponding to the frequency-indepdant noise term, S_I B.) S_I plotted as a function of photocurrent, showing a Fano Factor of $F \sim 1$

From these data, the Fano factor is found to be close to unity, as shown in Fig. 6b. We note that the magnitude of S_I in these devices is three orders of magnitude smaller (~10^{-25}) than in the previous samples.

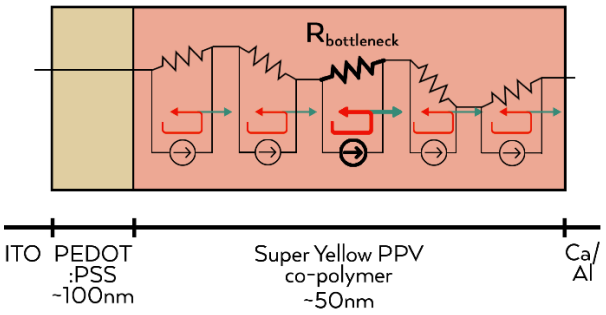

Fig. 7. Device structure and equivalent percolation network of the super yellow organic light emitting diodes. Shot noise generation is likely dominated by a single highly-resistive hopping site, giving rise to near-full-scale shot noise

The transport in polymeric organic devices occur via both intra-chain and inter-chain electron hopping along least resistive paths in a percolative network. If the barriers for all jumps are the same, the expected Fano factor is $F = 1/N$, where N is the number of hops the carriers take between electrodes [12]. Estimating the distance of a single hop to be ~1nm, and using a thickness of ~50nm, we would then expect F ~0.02, much lower than the observed value near unity. We can explain this by assuming that the percolation path is dominated by a single hop, shown in Fig. 7 as the resistor in bold, whose "bottle-neck" resistance dominates the entire percolative chain.

IV. Conclusion

In summary, the current cross-correlating technique allowed us to resolve mid-frequency noise contributions, namely shot noise and generation-recombination noise. Importantly, we see that the analysis of shot noise and the corresponding Fano factor can yield information about interfacial dynamics and charge transport. In particular, the shot noise associated with percolation in organic materials, such as the super yellow PPV co-polymer, hint at using this method to directly probe mesoscopic transport.

V. Acknowledgements

We wish to thank Dr. Christoph Böhme at the University of Utah for providing the super yellow PPV samples, Dr. Klaus Lips at the Helmholtz Zentrum Berlin for providing the silicon solar cell samples, and Dr. Kai Zhu at the U.S. National Renewable Energy Laboratory for providing the perovskite solar cell samples.

VI. References

[1] G. Bosman , *"Charge transport device parameters from noise measurements,"* IEEE Trans. Electron Devices, vol. 41, p. 2198, 1994.

[2] B. K. Jones, *"Low frequency noise spectroscopy,"* IEEE Trans. Electron Devices , vol. 41, p. 2188, Nov. 1994.

[3] G. Ferrari *et. al*, *"Current noise spectroscopy on mLPPP based organic light emitting diodes,"* Organic Electronics, vol. 3, pp. 33-42, 2002.

[4] L. Ke, X. Y. Zhao, R. S. Kumar, and S. J. Chua , *"Low-frequency noise measurement and analyses in organic light emitting diodes,"* IEEE Electron Device Lett., vol. 27, p. 555, 2006.

[5] E. G. Ioannidis *et. al*, *"Characterization of traps in the gate dielectric of amorphous and nanocrystalline silicon thin-film transistors by 1/f noise"*, J. Appl. Phys. , vol. 108, p. 106103, 2010.

[6] M. Sampietro, L. Fasoli, and G. Ferrari, *"Spectrum analyzer with noise reduction by cross-correlation technique on two channels,"* Rev. Sci. Instrum. **70**, 2520 (1999)

[7] G. Ferrari and M. Sampietro, *"Correlation spectrum analyzer for direct measurement of device current noise,"* Rev. Sci. Instrum. **73**, 2717 (2002)

[8] T.K. Djidjou, D.A. Bevans, S. Li, and A. Rogachev, *"Observation of shot noise in phosphorescent organic light-emitting diodes,"* IEEE Trans. Eletron. Devices, Vol. 61, No. 9, 3252 (2014)

[9] T.K. Djidjou, Y. Chen, T. Basel, J. Shinar, and A. Rogachev, *"Magnetic field enhancement of generation-recombination and shot noise in organic light emitting diodes,"* J. Appl. Phys. **117**, 115501 (2015)

[10] T.K.Djidjou, T. Basel, and A. Rogachev, *"Magnetic-field dependant differential capacitance of polymer diodes"*, Appl. Phys. Lett. **101** 093303 (2012)

[11] K. Davenport, T.K. Djidjou, S. Li, and A. Rogachev, *"Characterization of charge accumulation on multiple interfaces in phosphorescent organic light-emitting diodes"*, Org. Electron. **46** 166 (2017)

[12] A. N. Korotkov and K.K. Likharev, *"Shot noise suppresion in one-dimensional hopping,"* Phys. Rev. B **61** 15975 (2000)

[13] A.K. Jena *et. al*, *"Role of spiro-OMeTAD in performance deterioration of perovskite solar cells at high temperature and reuse of the perovskite films to avoid Pb-waste,"* J. Mater. Chem. A, **6**, 2219 (2018)

[14] J. Graeme, *"Photodiode Amplifiers: Op Amp Solutions"*, McGraw-Hill, 1996

This work has been funded by NSF grant no. DMR 1611421